Chemical Physics 441 (2014) 53–58

Contents lists available at ScienceDirect

Chemical Physics

journal homepage: www.elsevier.com/locate/chemphys

The effect of initial rotation in the $N(^2D) + H_2 \rightarrow NH(^3\Sigma^-) + H$ reaction

Ezman Karabulut [a,*], Emine Aslan [b], Jacek Kłos [c], Niyazi Bulut [d]

[a] Bitlis Eren University, Vocational School of Health Services, 13000 Bitlis, Turkey
[b] Ahi Evran University, Kaman Vocational School, 40100 Kirsehir, Turkey
[c] Department of Chemistry and Biochemistry, University of Maryland, College Park, MD 20742-2021, USA
[d] Firat University, Department of Physics, 23119 Elazig, Turkey

ARTICLE INFO

Article history:
Received 9 May 2014
In final form 3 July 2014
Available online 17 July 2014

Keywords:
Reaction probability
Integral cross sections
Rate constants

ABSTRACT

In this work, total reaction probabilities, integral cross sections and rate constants were calculated for selected initial rotational states of the H_2 molecule in the $N(^2D) + H_2$ reaction. Time dependent wave packet method combined with Centrifugal Sudden approximation was used and followed by a flux analysis on recently developed $NH_2(1^2A'')$ global potential energy surface. We also investigated the effect of the projection quantum number of the initial rotational state on the reactivity. Total reaction probabilities were calculated for all values of the total angular momentum, J, in the range from 0 to 40. The effects of the initial rotational excitation of the H_2 reactant and of its projection quantum number on the behavior of rate constants were studied. The reaction rate constants are compared with previously published experimental and theoretical results. It was found that the initial rotation and its projection have a big effect on the integral cross sections.

1. Introduction

The interaction of electronically excited atoms or molecules with other species in their ground electronic state has been a subject of a great interest in atmospheric chemistry, since they exhibit very long-lived complexes in the upper atmosphere. They are also interesting from the point of view of the environmental and combustion chemistry. The title reaction involves the metastable nitrogen atom in its first excited ^2D electronic state lying 2.38 eV above its ground ^4S state. The ^2D nitrogen, which is produced experimentally by a flash photolysis of N_2O in the vacuum ultraviolet [1] or two-photon dissociation of NO [2], has attracted the interest of astrophysicists and chemists. The high energy content of the complexes formed by electronically excited atoms enhances the reactivity in chemical reactions as these processes may be barrierless or can easily overcome reaction barriers [1,3–5]. Especially in Earth's thermosphere, the complexes that contain the excited nitrogen atom, form abundant metastable species with a long radiative lifetime [6]. There were many theoretical and experimental studies of the metastable nitrogen atom in the literature. Fell et al. studied the metastable $N(^2D)$ experimentally [1] for which also quenching rate constants using a series of gas quenchers such as N_2O, CO_2, H_2, CH_4 and O_2 were calculated.

The $N(^2D)+H_2$ reaction is an exothermic process ($\Delta H^0 = -29.4$ kcal/mol) characterized by a small early barrier (~2.3 kcal/mol) and by a deep potential well of 125.5 kcal/mol corresponding to $NH_2(1A'')$ molecule. Because of the existing discrepancies in the literature between experimental and theoretical results previous theoretical studies of this reaction were focused on constructions of accurate potential energy surface (PES). Particularly, in one of the studies, Kobayashi et al. [7] obtained *ab initio* PES for the NH_2 ground state by using first order configuration interaction (FOCI) calculations and used quasi-classical trajectory (QCT) method to test it. Afterwards, Pederson et al. [8] have reported the first global PES of the reaction by using the reproducing kernel Hilbert space interpolation method on a set of high level *ab initio* points. They have also performed detailed QCT calculations for isotopic variants of the title reaction. Employing the same PES, Balucani and coworkers [9] performed dynamical calculations via both quantum mechanical and statistical methods, and compared their theoretical results with the experiment. Subsequently, Ho et al. [10] improved the PES of Pederson and proposed new PES that was tested in QCT calculations. Their new PES is in good agreement with the other potentials in critical regions of the reaction. There are several dynamical studies in the literature demonstrating reliability of the above potentials used in such studies [11–13,54–55]. Experimental studies were generally focused on the reaction rate constants and rovibrational state distributions of the NH product obtained from both infrared chemiluminescence and laser-induced

* Corresponding author.
E-mail addresses: ekarabulut@beu.edu.tr (E. Karabulut), jklos@umd.edu (J. Kłos).

http://dx.doi.org/10.1016/j.chemphys.2014.07.003
0301-0104/

fluorescence (LIF) measurements. In the works of Dodd et al. [14] and Umemoto et al. [15–18], the nascent vibrational state distributions of ground NH molecule were examined in detail by LIF. However, the time-resolution of their experimental method prevented the monitoring of the rotational product distribution. Umemoto and coworkers determined vibrational and rotational state distributions of nascent NH molecule and its isotopic variant (ND) by two-photon dissociation of NO, as proposed by Slanger et al. [2]. Additionally, they examined the LIF spectrum of NH molecules formed in reaction of N with H_2.

Molecules that have deeply bound stable structures such as H_2O, CH_2, H_2S and NH_2 tend to preserve their geometry in the transition state region. For this particular reason, such reactions have been commonly studied with a statistical approach. Launay and Honvault [19] using statistical method examined distributions of squared scattering matrix elements for specific energies. At the same time, Manolopoulos et al. [20] has derived detailed statistical theory and confirmed it in comparison to fully quantum mechanical state-to-state integral cross sections of Honvault and Launay [21]. Balucani et al. [22] performed the comparison between experimental and theoretical results at collision energy of 15.9 kJ/mol. They used quantum mechanical and QCT methods to obtain differential cross sections for specific initial rotational quantum number of the reacting H_2 molecule. In another study, Defazio and Petrongolo [23] showed wave packet calculations using flux analysis. They obtained accurate reaction probabilities for $J = 0$, centrifugal sudden (CS) probabilities for $J > 0$ and cross sections by using simple J-shifting approximation, which works very well in a low energy region. Later, Varandas and Poveda [24] developed a single-sheeted double many-body expansion PES for this reaction and performed rigorous Close Coupling (CC) and CS calculations in collision energy range from 0 to 1 eV. Furthermore, they calculated cross sections and rate constants for specific initial rotational quantum numbers ($j = 0$–5) and compared with experimental and theoretical results reported before [13]. In another work by Balucani et al. [9], it was shown that the agreement between experimental and theoretical differential cross sections obtained with the PES of Pederson [8] for the collision energy of 15.9 kJ/mol is excellent. There is an important coupling between the product angular and translational energy distributions as explained in [9] and [22]. Castillo et al. [11] used PES of Ho et al. [10] and reported state-to-state reaction probabilities obtained in quantum mechanical real wave packet and QCT methods for the $J = 0$ partial wave. They used CS approximation to get the reaction probability results for partial waves J greater than zero. Integral cross sections were calculated by means of uniform J-shifting, refined J-shifting and standard J-shifting depending on vibrational state of a product molecule and as a function in a narrow energy range (0–0.25 eV) of collision energies. They found a good agreement between their results and available experimental measurements. Rao and Mahapatra et al. [12] used the same PES and reported quantum wave packet dynamics within Coupled States approximation to obtain initial state selected reaction probabilities, integral cross sections and rate constants. They additionally examined the vibrational energy levels of NH_2 by using Gaussian wave packet. Gonzalez-Lezana [25] reviewed integral cross sections and state-to-state reaction probabilities by combining some of the statistical quantum methods with experimental results of Umemoto [17] for vibrational state distributions of product molecule at collision energy of 165 meV. In another work for title reaction, Lin et al. [26] studied the Renner-Teller coupling between the two lowest-lying electronic states of NH_2. They observed the effect of the non-adiabatic coupling on the low-lying rovibrational states of the NH product and found substantial influence of the non-adiabaticity on the levels and as well on the differential and integral cross sections. In a recent study, Yang et al. [3] produced a new analytical form of the PES for the title reaction. The prospect of obtaining more accurate reaction probabilities in strong interaction region has encouraged this work. This PES is a function of all interatomic distances of the system and was constructed by performing intermolecular perturbation theory [27–30]. Using this analytic PES, Yang et al. [3] calculated total integral cross sections to compare them with QCT results obtained with PESs of Pederson and Ho for single collision energy of 0.165 eV. There are several other potentials available in the literature [56–58].

In this work, the Real Wave Packet (RWP) method was applied for the title reaction and combined with a flux method and Centrifugal Sudden (CS) approximation for $J > 0$ states. Initial state-selected integral cross sections and rate constants were obtained and compared with available experimental [31] and theoretical data. This paper is organized as follows. The theory outlined in Section 2 and the results are discussed in Section 3.

2. Method

In this work, the chemical reaction dynamics of the $N(^2D)+H_2$ reaction was investigated using a time-dependent wave packet method. Time dependent Schrödinger equation (TDSE) is given by,

$$i\hbar\frac{\partial\Psi(R,r,\gamma,t)}{\partial t} = \widehat{H}\Psi(R,r,\gamma,t) \tag{1}$$

where $\widehat{H}$ is the Hamilton operator of the system and ψ is the nuclear wave function, R is the distance from the N atom to the center-of mass of the H_2 molecule, r is the vibrational coordinate of the diatomic, γ is the angle formed between $\boldsymbol{R}$ and $\boldsymbol{r}$ vectors [32]. The wave function can be expanded as

$$\Psi(R,r,\gamma,t) = \widehat{U}(t)\Psi(0) = \exp\left(\frac{-i\widehat{H}t}{\hbar}\right)\Psi(R,r,\gamma,t=0) \tag{2}$$

The Hamiltonian expressed in reactant Jacobi coordinates (R, r, θ) for the body-fixed frame representation is

$$\widehat{H} = -\frac{\hbar^2}{2\mu_R}\frac{\partial^2}{\partial R^2} - \frac{\hbar^2}{2\mu_r}\frac{\partial^2}{\partial r^2} + \frac{\hbar^2}{2}\left(\frac{1}{\mu_R R^2} + \frac{1}{\mu_r r^2}\right)\hat{j}^2 + \frac{1}{2\mu_R R^2}\{J(J+1) - 2K^2\} + V(R,r,\gamma) + C^J_{K,K-1} + C^J_{K,K+1} \tag{3}$$

The last two terms in this equation are known as Coriolis coupling terms [33,34] defined as below:

$$C^J_{K,K\pm1} = -[J(J+1) - K(K\pm1)]^{1/2}[j(j+1) - K(K\pm1)]^{1/2}\lambda/2\mu_R R^2 \tag{4}$$

where λ is $\delta_{K,K+1}(1+\delta_{K0})^{1/2}$ and $\delta_{K,K-1}(1+\delta_{K1})^{1/2}$ and. In Eq. (3) μ_R is the reduced mass of N and H_2, μ_r is the reduced mass of H_2, J is the total angular momentum quantum number of the $N + H_2$ system and K in a body-fixed frame, the projection of total angular momentum $\mathbf{J}$ onto the Z-axis ($\mathbf{J}_z$) and the projection of the diatomic angular momentum $\mathbf{j}$ onto the Z-axis ($\mathbf{j}_z$). K may take the values in a following range:$0 \leqslant K \leqslant \min(J,j)$. In Eq. (4), different K-states in the wave function couple together. Therefore, more basis functions are required to store the exact information about the wave function. By increasing the number of grid points in the angular part we need more computer memory. Hence, here we used Centrifugal Sudden approximation for computing the reaction probabilities for $J > 0$. In the CS approximation, these off-diagonal elements are neglected and this considerably decreases the size of the Hamiltonian matrix [35]

$$\widehat{H} = -\frac{\hbar^2}{2\mu_R}\frac{\partial^2}{\partial R^2} - \frac{\hbar^2}{2\mu_r}\frac{\partial^2}{\partial r^2} + \frac{\hbar^2}{2}\left(\frac{1}{2\mu_R R^2} + \frac{1}{2\mu_r r^2}\right)\hat{j}^2 + \frac{1}{2\mu_R R^2} \times \{J(J+1) - 2K^2\} + V(R,r,\gamma) \tag{5}$$

Table 1
Parameters used in the calculations (all parameters given in atomic units).

Reactant scattering coordinate range:	R_{min} = 0.0; R_{max} = 17.0
Number of grid points in R:	340
Diatomic coordinate range:	r_{min} = 0.0; r_{max} = 17.0
Number of grid points in r:	440
Number of angular basis functions:	200
Center of initial wave packet:	R_0 = 12.0
Initial translational kinetic energy/eV:	E_c = 0.25
Analysis point:	13.0
Number of Chebyshev iterations:	30,000

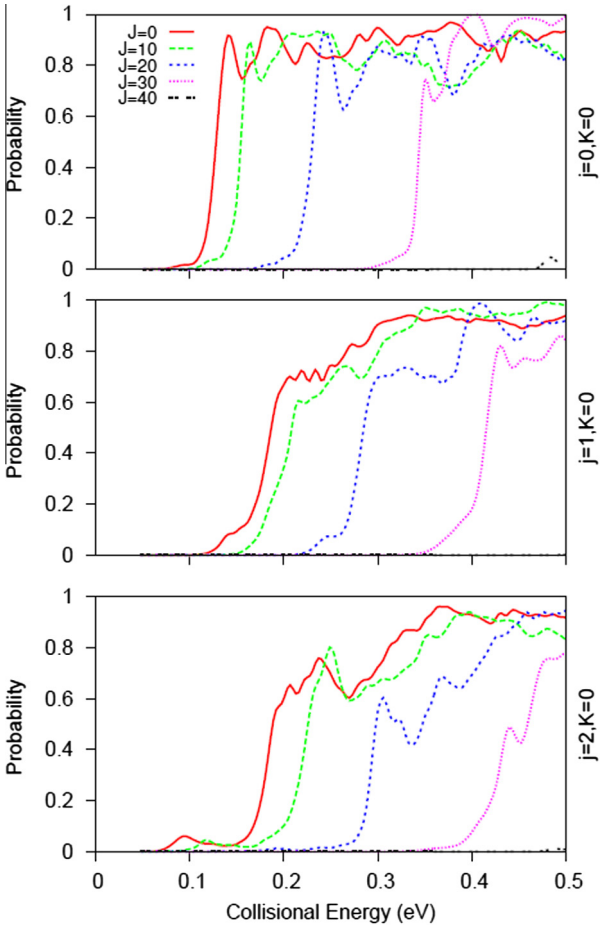

Fig. 1. Total reaction probabilities for selected values of the total angular momentum quantum number J as a function of collision energy for initial j = 0,1 and 2 rotational states of H_2 with projection K = 0.

After sufficient long time propagation we can extract the total reaction probability and the total reaction cross sections using a flux analysis method. This method takes the wave packet at the analysis line (see Table 1) as an input. Therefore, the probabilities were calculated for the wave packet in the outgoing channel along the analysis line [36–46]. The reaction probability for $J > 0$,

$$P_i^{JK}(E) = \frac{\hbar}{\mu_R} Im\left[\left\langle \psi(R, r_d, \gamma, E) \middle| \frac{\partial \psi(R, r_d, \gamma, E}{\partial r} \right\rangle\right] \quad (6)$$

where E is collision energy, r_d shows analysis line $r = r_d$ and

$$\psi(R, r_d, \gamma, E) = \frac{1}{\sqrt{2\pi}} \int_{-\infty}^{+\infty} \psi(R, r, \gamma, t) e^{-Et/\hbar} dt|_{r=r_d} \quad (7)$$

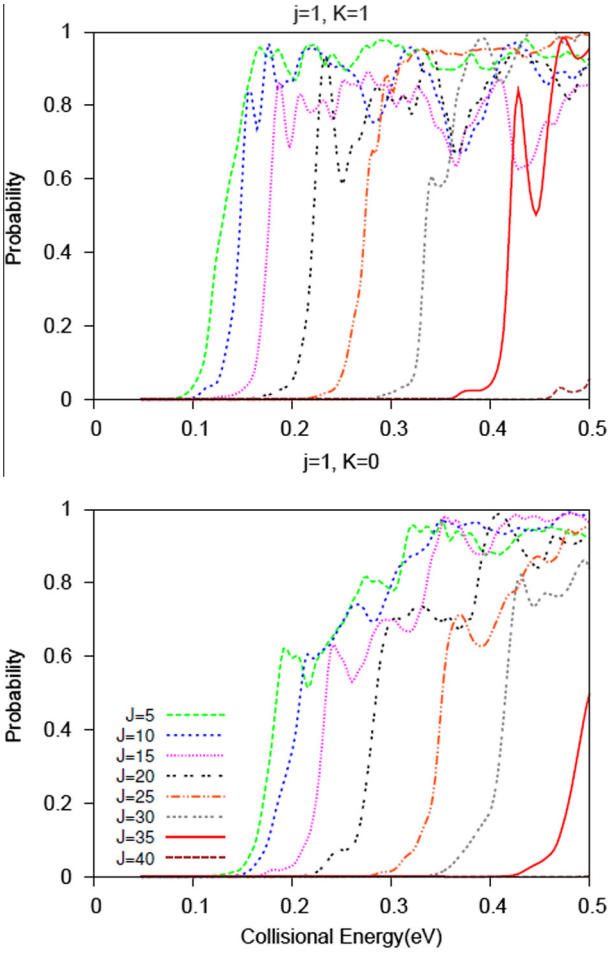

Fig. 2. Total reaction probabilities for selected values of the total angular momentum quantum number J for K = 1 (top panel) and K = 0 (bottom panel) of j = 1 initial rotational state.

is the Fourier transform of the time-dependent wave function $\psi(R, r_d, \gamma, E)$ at given analysis line $r = r_d$. The total initial state-selected reaction cross sections and rate coefficients

$$\sigma_{all \leftarrow vj}^{tot}(E) = \frac{1}{(2j+1)} \frac{\pi}{k_{vj}^2} \sum_J (2J+1) P_J^{react}(E) \quad (8)$$

$$k_{vj}(T) = \left(\frac{8}{\pi \mu_R (k_B T)^3}\right)^{1/2} \int_0^{\infty} E \sigma_{vj}(E) e^{-E/k_B T} dE \quad (9)$$

where k_B is Boltzmann constant.

3. Results and discussions

In order to get converged results of reaction probabilities the parameters in Table 1 used.

Fig. 1 shows reaction probabilities for several values of the total angular momentum quantum number J. The reaction probabilities are shown for three selected values of the initial H_2 rotational quantum number from 0 to 2 in collision energy range from 0 to 0.5 eV. The reaction probabilities sharply rise near the threshold at $j = 0$, **J = 0**, and increase only slightly when initial rotational state increases from $j = 0$ to $j = 2$. For the J > 0 states this increase is not so sharp. It is interesting to note that the trend of the total reaction probability for all considered values of initial j's exhibits an increase (rapid increase for the $j = 0$) and then reaching oscillatory

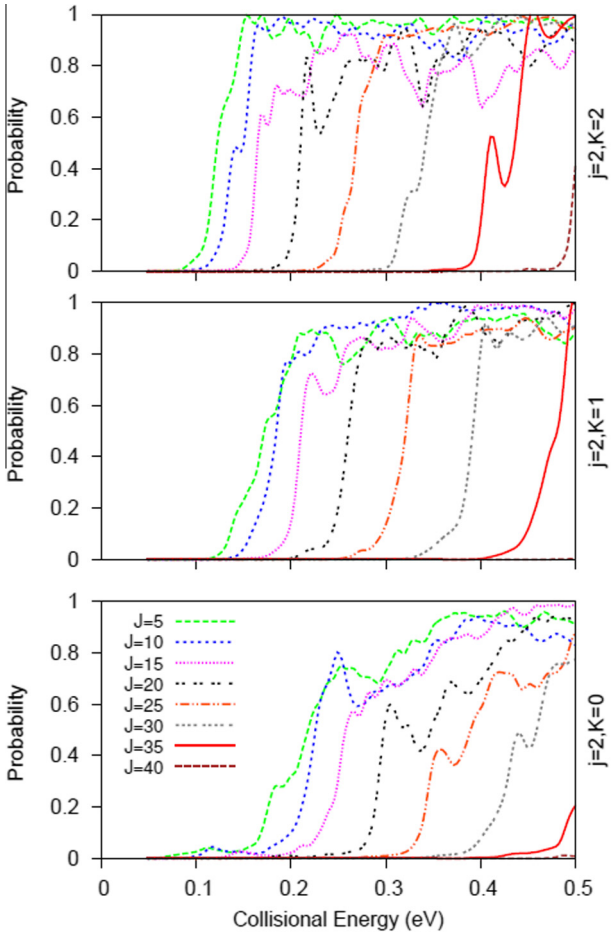

Fig. 3. Total reaction probabilities for selected values of the total angular momentum quantum number J for the relevant K values of the $j = 2$ initial rotational state.

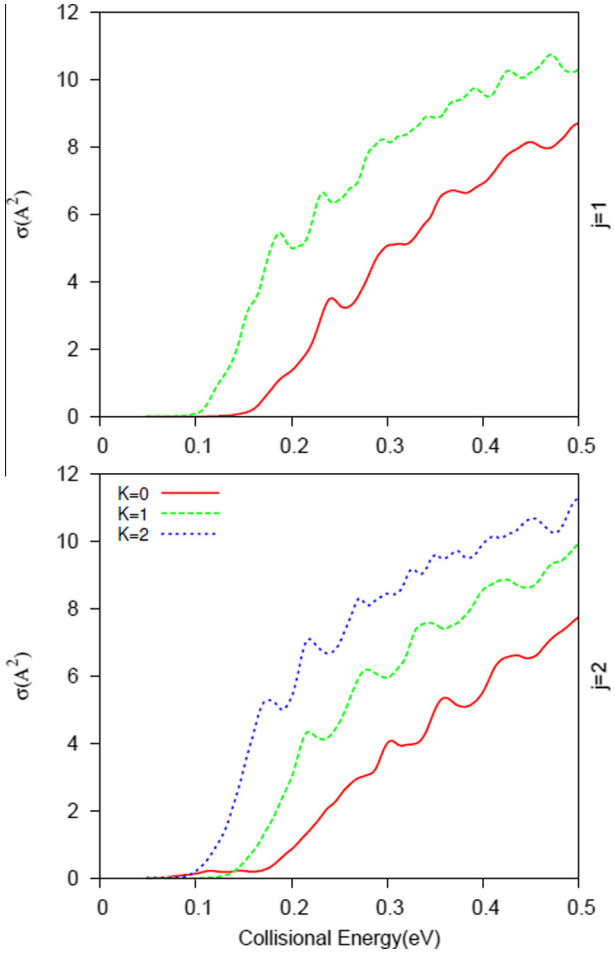

Fig. 4. Integral cross sections for K states corresponding to $j = 1$(top panel) and $j = 2$ (bottom panel).

plateau for higher collision energies. Similar behavior was also found in a work by Lin et al. [26]. The reactivity is in general the largest for all partial waves shown in the figure for the $j = 0$ initial state. A sharp increase in the threshold region is less pronounced when the j value increases and the reactivity shifts towards higher collision energies owing to the centrifugal barrier. The behavior of the reaction probabilities at the region of the threshold for selected initial rotational states can be also seen for other reactions such as Ca + HCl [47,48], its reverse and H + FLi [49–51]. The oscillations in reaction probabilities observed in Fig. 1 are of smaller amplitude than those for different PESs of [11,24] for the same reaction.

Reaction probabilities for different values of the projection quantum number K for $j = 1$ are shown in Fig. 2 as functions of collision energy. The top and bottom panels of the figure are for the $K = 1$ and $K = 0$, respectively. When the projection quantum number K increases the reaction probabilities shift to lower energies and oscillatory structures are more explicit. Besides, the total reaction probabilities display a sharp rise near the threshold for every J with increasing K. Reaction probabilities shift to high collision energies with increasing J because of the centrifugal barrier. The effect of K for $j = 2$ is displayed in Fig. 3. Similar conclusions can be drawn here as before for Fig. 2.

Fig. 4 shows integral cross sections as a function of collision energy for the relevant K values that belong to $j = 1$ (top panel) and $j = 2$ (bottom panel) initial rotational states. Integral cross sections have been computed considering the total reaction probabilities for all J's in collision energy range from 0.05 to 0.5 eV. The effect of the projection of initial rotational quantum number (K) shifts the reactivity towards the low energy region because of the $-2K^2$ factor, and decreases centrifugal barrier as expected.

Reactive integral cross sections increase gradually with K from the threshold in the considered range of energy. One can conclude that there is large enhancement effect on the reactivity when projection quantum number K increases.

Fig. 5 presents integral cross sections averaged on the relevant K values for specific initial rotational ($j = 0$–2) quantum states. Although the reaction probabilities in Fig. 1 have different threshold energies for various values of j due to the barrier in the entrance channel region, integral cross sections for averaged K display nearly the same threshold. Here as well the oscillatory behavior is noticeable for all initial j's and it persists from threshold up to 0.5 eV of collision energy. The present results when compared with that of Ref. [11], have smaller cross sections and less pronounced oscillations.

In Fig. 6 rate constants for the three values of the initial rotational state of H_2 are shown in a temperature range of 200–500 K. The experimental [31] and theoretical [13] values that are available in the literature are also shown. The experimental and theoretical rate constants obtained in this studies at room temperature for $j = 0$ are 2.28×10^{-12} [31] and 2.18×10^{-12} $cm^3\ s^{-1}$, respectively. The experimental rate constant is averaged on the Boltzmann populations at a given temperature. Note that in the low temperature region present calculations give lower rates in a good accord with experimental results.

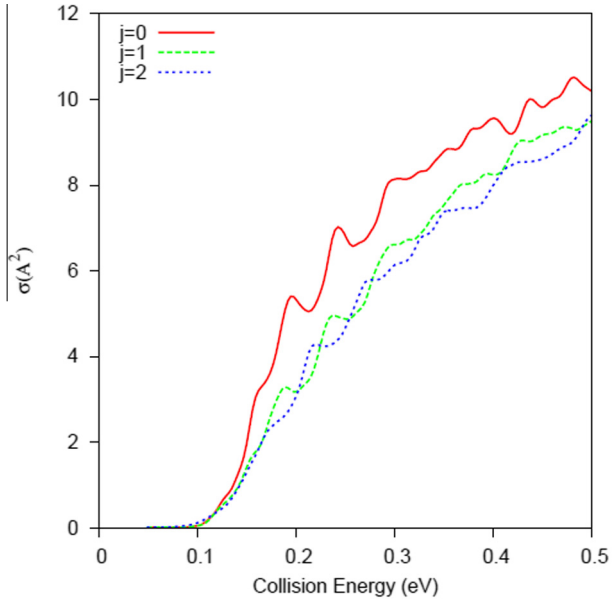

Fig. 5. Integral cross sections averaged on the relevant K values for 0, 1 and 2 values of initial j.

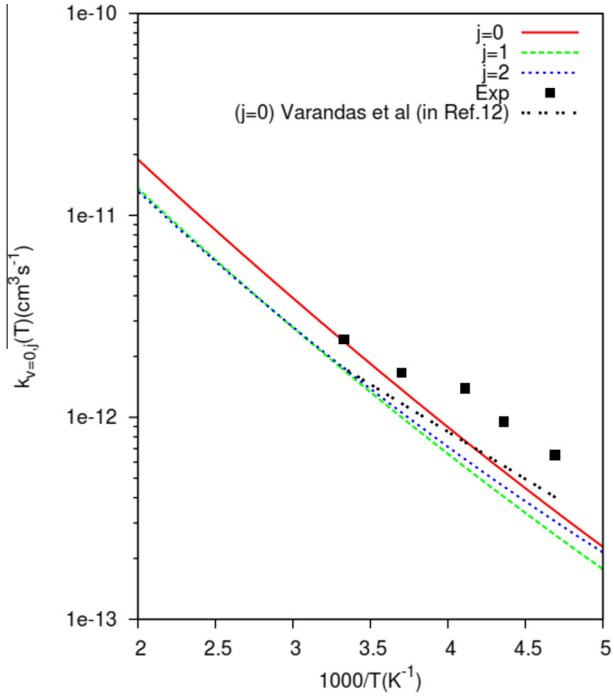

Fig. 6. Reaction rate constants related to CS results for $j = 0$, 1 and 2 initial H_2 rotational states. The figure also shows other theoretical and experimental results for $j = 0$ initial state.

Fig. 7 presents graphical representation of the origins of the enhancement of the reactivity with increasing projection quantum number K. The N + H_2 insertion reaction is characterized by a small early barrier (~0.84 meV) in the C_{2v} approach of the nitrogen towards the hydrogen [10]. In the case when the absolute value of the projection quantum number K is equal to j, the N + H_2 complex has increased chances to react due to the more favorable orientation for the insertion process. This is achieved for the Propeller type of H_2 rotation shown in panel (c) of the figure. For the other two cases with $K = 0$ (Frisbee and Cartwheel type rotations of H_2, see panel (a) and (b) of Fig. 7, respectively) the nitrogen will experience more chances of head-on collisions that are less reactive as chances for the insertion process are decreased. Similar rotational orientation arguments have allowed for a simple explanation of different propensities in product distributions of O + H_2 reaction [52,53].

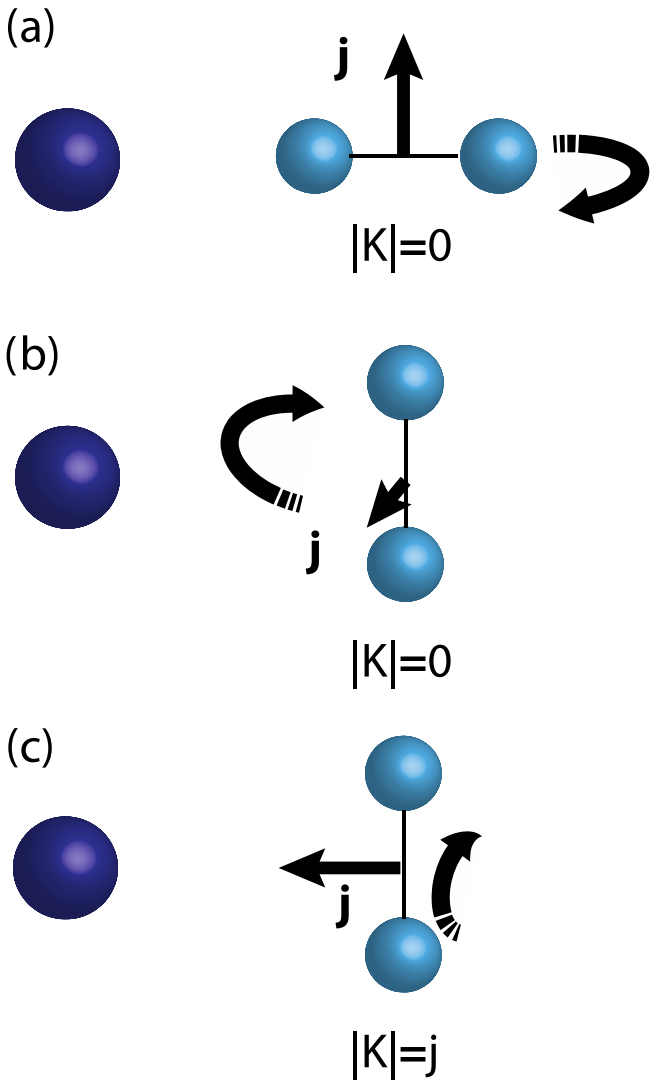

Fig. 7. In panel a) the helicopter rotational motion of the H_2 molecule with the rotational angular momentum j perpendicular to the body fixed Z-axis with projection $K = 0$, b) cartwheel rotational motion with the rotational angular momentum $\boldsymbol{j}$ perpendicular to the body fixed Z-axis with $K = 0$ and c) propeller type rotation with the initial rotational angular momentum $\boldsymbol{j}$ parallel to the body fixed Z-axis with $|K|=j$. The blue sphere represents the nitrogen atom. (For interpretation of the references to colour in this figure legend, the reader is referred to the web version of this article.)

4. Conclusions

In this work, a time dependent wave packet method within Centrifugal Sudden approximation followed by a flux analysis was applied to the N(^{2}D)+H_2 reaction. We calculated total reaction probabilities, integral cross sections and rate constants at several selected initial rotational states of the H_2 molecule. There is good agreement found between the experimental and calculated rate constant at room temperature considering that the Centrifugal Sudden approximation for total reaction probabilities has been employed. Total reaction probabilities were calculated for all

values of the total angular momentum without using any interpolation method. It is found that the initial rotational quantum number of the H_2 molecule and its projection (K) has a noticeable effect on the integral cross sections. This effect is probably due to the CS approximation, because it was not found in previous coupled-channel studies.

Conflict of interest

The authors declare no competing financial interest.

Acknowledgements

This work has received financial support from the Scientific and Technological Research Council of Turkey for TR-Grid facilities through a project (TBAG-112T827).

References

[1] B. Fell, I.V. Rivas, D.L. McFadden, J. Phys. Chem. 85 (1981) 224.
[2] L.E. Jusinski, G.E. Gadd, G. Black, T.G. Slanger, J. Chem. Phys. 90 (1989) 4282.
[3] C.-L. Yang, L.-Z. Wang, M.-S. Wang, X.-G. Ma, J. Phys. Chem. A 117 (2013) 3.
[4] H. Umemoto, K. Sugiyama, S. Tsunashima, S. Sato, Bull. Chem. Soc. Jpn. 58 (1985) 3076.
[5] T. Suzuki, Y. Shihira, T. Sato, H. Umemoto, S. Tsunashima, J. Chem. Soc. Faraday Trans. 89 (1993) 995.
[6] P. Casavecchia, N. Balucani, M. Alagia, L. Cartechini, G.G. Volpi, Acc. Chem. Res. 32 (1999) 503.
[7] H. Kobayashi, T. Takayanagi, K. Yokoyama, T. Sato, S. Tsunashima, J. Chem. Soc. Faraday Trans. 91 (1995) 3771.
[8] L.A. Pederson, G.C. Schatz, T.-S. Ho, T. Hollebeek, H. Rabitz, L.B. Harding, G. Lendvay, J. Chem. Phys. 110 (1999) 9091.
[9] N. Balucani, P. Casavecchia, L. Banares, F.J. Aoiz, T. Gonzalez-Lezana, P. Honvault, J.-M. Launay, J. Phys. Chem. A 110 (2006) 817.
[10] T.S. Ho, H. Rabitz, F.J. Aoiz, L. Banares, S.A. Vazquez, L.B. Harding, J. Chem. Phys. 119 (2003) 3063.
[11] J.F. Castillo, N. Bulut, L. Banares, F. Gogtas, Chem. Phys. 332 (2007) 119.
[12] B.J. Rao, S. Mahapatra, J. Chem. Phys. 127 (2007) 244307.
[13] T.-S. Chu, K.-L. Han, A.J.C. Varandas, J. Phys. Chem. A 110 (2006) 1666.
[14] J.A. Dodd, S.J. Lipson, D.J. Flanagan, W.A.M. Blumberg, J. Chem. Phys. 94 (1991) 4301.
[15] H. Umemoto, N. Terada, K. Tanaka, J. Chem. Phys. 112 (2000) 13.
[16] H. Umemoto, Y. Kimura, T. Asai, Bull. Chem. Soc. Jpn. 70 (1997) 2951.
[17] H. Umemoto, T. Asai, Y. Kimura, J. Chem. Phys. 106 (1997) 12.
[18] H. Umemoto, K.-I Matsumoto, J. Chem. Phys. 104 (1996) 9640.
[19] P. Honvault, J.-M. Launay, Chem. Phys. Lett. 329 (2000) 233.
[20] E.J. Rackham, F. Huarte-Larranaga, D.E. Manolopoulos, Chem. Phys. Lett. 343 (2001) 356.
[21] P. Honvault, J.-M. Launay, J. Chem. Phys. 111 (1999) 6665.
[22] N. Balucani, L. Cartechini, G. Capozza, E. Segoloni, P. Casavecchia, G.G. Volpi, F.J. Aoiz, L. Banares, P. Honvault, J-M. Launay, Phys. Rev. Lett 89 (2002) 1.
[23] P. Defazio, C. Petrongolo, J. Theor. Comput. Chem. 2 (2003) 547.
[24] A.J.C. Varandas, L.A. Poveda, Theor. Chem. Acc. 116 (2006) 404.
[25] T. Gonzalez-Lezana, Int. Rev. Phys. Chem. 26 (2007) 29.
[26] S.-Y. Lin, H. Guo, B. Jiang, S. Zhou, D. Xie, J. Phys. Chem. A 114 (2010) 9655.
[27] M.P. Hodges, A.J. Stone, E.C. Lago, J. Phys. Chem. A 102 (1998) 2455.
[28] J.S. Winn, J. Chem. Educ. 58 (1981) 37.
[29] Y. Changfang, W. Zhivei, J. Nat. Sci. 13 (2008) 212.
[30] A. Aguado, C. Tablero, M. Paniagua, Comput. Phys. Commun. 134 (2001) 97.
[31] H. Umemoto, N. Hachiya, E. Matsunaga, A. Suda, M. Kawasaki, Chem. Phys. Lett. 296 (1998) 203.
[32] D.M. Neumark, A.M. Wodtke, G.N. Robinson, C.C. Hayden, K. Shobatake, R.K. Sparks, J. Chem. Phys. 82 (1985) 3067.
[33] P. Mcguire, D.J. Kouri, J. Chem. Phys. 60 (1974) 2488.
[34] T. Gonzalez-Lezana, O. Roncero, P. Honvault, J.M. Launay, N. Bulut, F.J. Aoiz, L. Banares, J. Chem. Phys. 125 (2006) 094314.
[35] R.T. Pack, J. Chem. Phys. 60 (1974) 633.
[36] N. Balakrishnan, C. Kalyanaraman, N. Sathyamurthy, Phys. Rep. 280 (1997) 79.
[37] J.Z.H. Zhang, J.Q. Dai, W. Zhu, J. Phys. Chem. A 101 (1997) 2746.
[38] T.S. Chu, K.-L. Han, M. Hankel, G.G. Balint Kurti, J. Chem. Phys. 126 (2007) 214303.
[39] T.S. Chu, R.F. Lu, K.-L. Han, X.N. Tang, H.F. Xu, C.Y. Ng, J. Chem. Phys. 112 (2005) 244322.
[40] L. Yao, L.P. Ju, T.S. Chu, K.-L. Han, Phys. Rev. A 74 (2006) 062715.
[41] T.S. Chu, Y. Zhang, K.-L. Han, Int. Rev. Phys. Chem. 25 (2006) 201.
[42] T.S. Chu, K.-L. Han, J. Phys. Chem. A 109 (2005) 2050.
[43] T.X. Xie, Y. Zhang, M.Y. Zhao, K.-L. Han, Phys. Chem. Chem. Phys. 5 (2003) 2034.
[44] Y. Zhang, T.X. Xie, K.-L. Han, J.Z.H. Zhang, J. Chem. Phys. 119 (2003) 12921.
[45] D. Neuhauser, M. Bear, R.S. Hudson, D.J. Kouri, Comp. Phys. Comunn. 63 (1991) 460.
[46] A.J. Meijer, E.M. Goldfield, S.K. Gray, G.G. Balint-Kurti, Chem. Phys. Lett. 293 (1998) 270.
[47] C. Sanz, A.V.D. Avoird, O. Roncero, J. Chem. Phys. 123 (2005) 064301.
[48] G. Verbockhaven, C. Sanz, G.C. Groenenboom, O. Roncero, A.V.D. Avoird, J. Chem. Phys. 122 (2005) 204307.
[49] W. Zhu, D. Wang, J.Z.H. Zhang, Theor. Chem. Acc. 96 (1997) 31.
[50] P.F. Weck, N. Balakrishnan, J. Chem. Phys. 122 (2005) 234310.
[51] P.F. Weck, N. Balakrishnan, J. Chem. Phys. 122 (2005) 154309.
[52] M.H. Alexander, Nat. Chem. 5 (2013) 253.
[53] S.A. Lahankar, J. Zhang, K.G. McKendrick, T.K. Minton, Nat. Chem. 5 (2013) 315.
[54] P. Gamallo, P. Defazio, M. Gonzalez, C. Petrongolo, J. Chem. Phys. 129 (2008) 244307.
[55] E. Karabulut, E. Aslan, N. Bulut, Commun. Comput. Chem. 2 (2014) 36.
[56] Z.-W. Qu, H. Zhu, R. Schinke, L. Adam, W. Hack, J. Chem. Phys. 122 (2005) 204313.
[57] S. Zhou, D. Xie, S.Y. Lin, H. Guo, J.Chem. Phys. 128 (2008) 224316.
[58] S. Zhou, Z. Li, D. Xie, S.Y. Lin, H. Guo, J.Chem. Phys. 130 (2009) 184307.